

New Dataset and Methods for Fine-Grained Compositional Referring Expression Comprehension via Specialist-MLLM Collaboration

Xuzheng Yang^{*1}, Junzhuo Liu^{*1}, Peng Wang^{†1}, Guoqing Wang¹, *Member, IEEE*, Yang Yang¹, *Senior Member, IEEE*, and Heng Tao Shen¹², *Fellow, IEEE*

¹University of Electronic Science and Technology of China ²Tongji University

Abstract—Referring Expression Comprehension (REC) is a foundational cross-modal task that evaluates the interplay of language understanding, image comprehension, and language-to-image grounding. It serves as an essential testing ground for Multimodal Large Language Models (MLLMs). To advance this field, we introduce a new REC dataset characterized by two key features. First, it is designed with controllable difficulty levels, requiring multi-level fine-grained reasoning across object categories, attributes, and multi-hop relationships. Second, it incorporates negative text and images generated through fine-grained editing and augmentation, explicitly testing a model’s ability to reject scenarios where the target object is absent—an often-overlooked yet critical challenge in existing datasets. To address fine-grained compositional REC, we propose novel methods based on a Specialist-MLLM collaboration framework, leveraging the complementary strengths of these models: Specialist Models excel at simpler tasks with high efficiency, while MLLMs are better suited for complex reasoning. Building on this synergy, we introduce two collaborative strategies. The first, Slow-Fast Adaptation (SFA), employs a routing mechanism to adaptively delegate simple tasks to Specialist Models and complex tasks to MLLMs. Additionally, common error patterns in both models are mitigated through a simple yet effective target-refocus strategy. The second, Candidate Region Selection (CRS), generates multiple bounding box candidates for the target object based on Specialist Model and uses the advanced reasoning capabilities of MLLMs to identify the correct target. Extensive experiments on our proposed dataset and other challenging compositional REC benchmarks validate the effectiveness of our approaches. The SFA strategy achieves a superior trade-off between localization accuracy and efficiency, and the CRS strategy significantly boosts the performance of both Specialist Models and MLLMs. We aim for this work to offer valuable insights into solving complex real-world tasks by strategically combining existing tools for maximum effectiveness, rather than reinventing them.

Index Terms—Referring Expression Comprehension (REC), Multimodal Large Language Models (MLLMs), Specialist Model, reasoning

I. INTRODUCTION

REFERRING Expression Comprehension (REC) is a fundamental vision-to-language task that aims to localize a target object described by a natural language expression [1].

X. Yang and J. Liu contributed equally to this work. P. Wang is the corresponding author.

Successfully addressing this task requires visual understanding, linguistic comprehension, and language-to-image grounding, making it an ideal testbed for Multimodal Large Language Models (MLLMs). REC has broad applications in assistive AI systems, such as a robotic assistant identifying “the red cup next to the coffee make” in a cluttered kitchen or an AI-powered medical tool pinpointing a specific lesion in radiology scans based on textual descriptions from doctors.

To advance Referring Expression Comprehension research and its real-world applications, datasets tailored for Multimodal Large Language Models (MLLMs) are essential. Traditional REC benchmarks such as RefCOCO, RefCOCO+, and RefCOCog [2]–[4] lack considerations for compositional reasoning, allowing models to perform well without truly understanding linguistic structure—or in some cases, even without relying on the expression itself [5], [6]. Moreover, most existing datasets do not include negative samples, where the target object is absent from the image. This omission is critical, as real-world REC scenarios often require models to reject incorrect object proposals when the described entity is not present. The lack of such negative examples limits the robustness of current REC models, making them prone to false positives.

To address these limitations, we introduce FineCops-Ref, a benchmark specifically designed to enhance fine-grained reasoning in REC. Our dataset incorporates controlled difficulty levels, compelling MLLMs to reason across object categories, attributes, and multi-hop relationships. The difficulty levels are categorized based on the number of attributes and relationships necessary for accurately localizing the target object. Specifically, if an image contains only one possible target, the difficulty level is set to 1, regardless of the complexity of the expression. When there are multiple objects of the same category as the target object in the image, and they can be distinguished by a single attribute or relationship, the difficulty level is assigned as 2. Conversely, if the model is required to interpret two or more relationships and attribute dependencies, the difficulty level is set to 3. Beyond compositional complexity, FineCops-Ref introduces negative samples carefully constructed through meticulous editing. These samples evaluate model resilience against misalignments and

hallucinations, providing a more rigorous assessment of their true visual grounding capabilities. By addressing both compositional reasoning and negative sample inclusion, FineCops-Ref establishes a more realistic and challenging benchmark for advancing REC research in the MLLM era.

While MLLMs demonstrate strong generalization and reasoning abilities, they often struggle with fine-grained localization and compositional grounding, particularly when precise object differentiation is required. In contrast, Specialist Models, which are typically lightweight and trained for specific vision tasks, excel in efficient and accurate low-level perception but lack the broad contextual reasoning capabilities of MLLMs. Given their complementary strengths, an effective solution is to leverage both models strategically—assigning simpler, perception-driven tasks to Specialist Models while reserving MLLMs for complex reasoning. This collaborative approach not only enhances accuracy and robustness but may also improve computational efficiency, as MLLMs are invoked only when necessary.

Motivated by this insight, we propose two Specialist-MLLM collaboration strategies to enhance REC performance. The first strategy, Slow-Fast Adaptation (SFA), introduces an adaptive task routing mechanism that dynamically assigns simpler, detection-oriented tasks to lightweight Specialist Models, while delegating complex tasks requiring compositional reasoning to MLLMs. This adaptive and flexible collaboration not only improves efficiency but, more importantly, enhances overall REC performance. Additionally, we identify common error patterns in both types of models, particularly their tendency to mistakenly identify objects not belonging to the described category. To mitigate this issue, we propose a simple yet effective target-refocus strategy, which obviously reduces localization confusion for both Specialist Models and MLLMs. Notably, the SFA strategy is entirely training-free, making it highly practical for real-world applications. The second strategy, Candidate Region Selection (CRS), aims to improve recall and precision by generating multiple object candidates using Specialist Models, followed by leveraging MLLMs’ reasoning capabilities to select the correct target. While MLLMs inherently possess reasoning capacity, they are not explicitly trained to approach selection tasks as generative problems, limiting their effectiveness in such scenarios. To address this, we conduct instruction tuning on external datasets, ensuring that MLLMs can effectively address selection tasks while avoiding knowledge leakage. This instruction tuning process generalizes well across various REC datasets.

Experiments on three compositional REC datasets demonstrate that our Specialist-MLLM collaboration strategies significantly enhance the performance of both existing Specialist Models and MLLMs, highlighting the generalizability of our approach. Beyond achieving superior performance, we aim for this work to provide valuable insights into solving complex real-world tasks by strategically leveraging existing models for maximum effectiveness, rather than reinventing them. This aligns with the broader trend of rapidly evolving LLM-based agents, emphasizing the importance of optimizing their potential to tackle challenging tasks efficiently.

The preliminary version of this work was published in [7].

In this paper, we made significant extensions. While the FineCops-Ref benchmark was introduced in [7], this work goes further by proposing two Specialist-MLLM collaboration strategies to effectively tackle the fine-grained compositional REC task, both within FineCops-Ref and across other external benchmarks. Additionally, we present more comprehensive experiments and analyses, providing a more self-contained and in-depth exploration of the fine-grained compositional REC task.

II. RELATED WORKS

A. Benchmarking Referring Expression Comprehension

Referring Expression Comprehension (REC) is a vision-language task where models must localize a target object in an image based on a natural language referring expression, requiring compositional understanding of attributes (e.g., color, size), spatial relationships, and object categories to disambiguate the referent from other entities. While early benchmarks like RefCOCO/+g [2]–[4] established foundational evaluation protocols, subsequent analyses revealed critical limitations. For instance, [5] and [6] demonstrated that models could exploit dataset biases rather than genuinely parse linguistic structure: [6] found that up to 83.7% of RefCOCOg test instances could be solved via keyword matching or visual feature dominance, bypassing compositional reasoning. To address this, [6] introduced Ref-Adv, a dataset where perturbed expressions refer to alternate objects, forcing models to engage with linguistic structure. Subsequent efforts have prioritized compositional reasoning. CLEVR-Ref+ [8] is a synthetic dataset emphasizing relationships, attributes, and linguistic logic. Cops-Ref [9] and Ref-Reasoning [10] use GQA scene graphs [11] and rule-based methods to create large-scale compositional referring expression comprehension datasets in real-world scenarios. Cops-Ref additionally introduces distracting images based on attributes, relationships, and target names. Recent benchmarks like GITM-MR [12] explore mismatched relationship in the REC task. ARPGrounding [13] evaluates the model’s compositional reasoning ability by constructing referring expression pairs that target distinct objects of the same category within a single image, differentiated solely through their attributes or relational contexts. RefEgo [14] and OmniLabel [15] consider out-of-distribution scenarios where referred targets do not exist in the image.

Building on these advances, we propose a new REC benchmark that more comprehensively assesses the compositional reasoning abilities of multimodal models. Our dataset incorporates controlled difficulty levels, compelling MLLMs to reason across object categories, attributes, and multi-hop relationships. Crucially, we also introduce negative text and image samples to evaluate model resilience against misalignments and hallucinations, providing a more thorough assessment of their true visual grounding capabilities. By simultaneously addressing compositional reasoning and incorporating negative samples, FineCops-Ref establishes a more realistic and challenging benchmark for advancing REC research in the MLLM era.

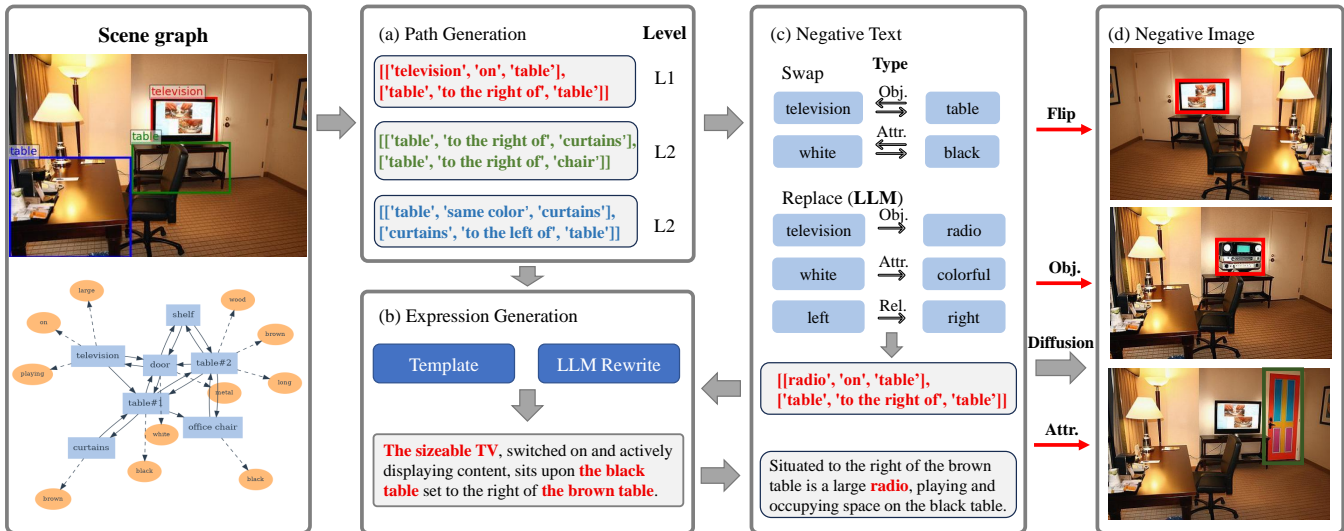


Fig. 1: The data construction pipeline of FineCops-Ref. Given an image, we first generate paths based on its scene graph. Then, we fill paths into templates and obtain the positive referring expression through LLM rewriting. Meanwhile, we utilize LLM to generate negative expressions, and based on this, we employ diffusion model to create fine-grained editing negative images.

B. Specialist REC Models

Early Specialist Models [16]–[24] typically employed pre-trained detectors to generate proposals and locate targets through text-to-region matching. Subsequent approaches transitioned to ViT-based architectures, typically adopting one-stage designs [25]–[28]. Recent advancements [29]–[32] have shifted towards DETR-based [33] frameworks, utilizing encoder-decoder architectures for multimodal fusion and generating target bounding boxes through object queries. Specifically, MDETR [29] pioneered the integration of free-form text with DETR, developing an end-to-end modulated detector capable of identifying objects in images based on raw text queries. UNINEXT [30] implemented Deformable DETR [34], proposing a universal instance perception model. Grounding-DINO [31], building upon the advanced DINO framework [35], enhanced DINO by incorporating vision-language modality fusion at multiple stages. [36] explored the utilization of hard negative samples during training. More recent models, such as OneRef [37] and SimVG [38] have streamlined the architecture by eliminating complex integration designs and redundant parameters through the implementation of modality-shared feature spaces, employing a unified multimodal encoder. Specialist REC models, typically lightweight and specifically trained for vision tasks, excel in efficient and accurate low-level perception. However, they generally lack broad contextual reasoning capabilities, which limits their performance on complex REC tasks.

C. Multimodal Large Language Models for REC

Unlike Specialist REC models, which usually treat REC as a bounding box regression task, MLLMs often formulate the bounding box prediction as a text generation problem, outputting bounding box coordinates in an autoregressive man-

ner. Recent MLLMs [39]–[46] have leveraged the powerful capabilities of LLMs through zero-shot or instruction tuning methods to address complex REC tasks. These MLLMs also known as grounding MLLMs [1]. Shikra [39] is an early model to support region-level input and understanding. Grounding-GPT [41] employs a coarse-to-fine training strategy to enhance model’s semantic awareness. CogVLM [43] incorporated a visual expert module in each transformer layer to enable dual fusion between vision and language features. CogCoM [44] introduced Chain of Manipulations, encouraging MLLMs to generate responses through evidential visual reasoning. Regarding visual modules, some methods, such as GLaMM [47] and LLaVA-Grounding [48], integrate additional visual components, while others, including Groma [49], VisualCoT [50], Ferret [40], and CoVLM [51], extract regional features as supplementary inputs. Recently, generalist MLLMs, such as Qwen2-VL [52] and InternVL 2.5 [53], have demonstrated significant advancements in grounding capabilities while maintaining strong reasoning performance, achieved through enhanced model architectures, carefully curated datasets, and optimized training strategies.

MLLMs demonstrate superior generalization and reasoning capabilities compared to Specialist Models, making them particularly well-suited for complex REC tasks demanding deeper contextual understanding. However, MLLMs inherit significant computational burdens from two key aspects. First, they rely on LLMs which possess substantially more parameters than Specialist Models. Second, the attention mechanisms used by MLLMs exhibit quadratic scaling of computational complexity. This scaling is further exacerbated by the increased input length resulting from the integration of numerous visual tokens (e.g., image patches) with textual tokens.

TABLE I: Comparison between the proposed benchmark and other REC benchmarks. Unconstrained indicates the final expression is not constrained by the templates. Cops. indicates compositional reasoning. On the right hand side, the test set count of each benchmark is listed.

Benchmark	Unconstrained	Cops.	Difficulty level	Neg. text	Neg. image	Positive		Negative	
						Expression	Image	Expression	Image
RefCOCO [3]	✓					10,752	-	-	-
RefCOCO+ [3]	✓					10,615	-	-	-
RefCOCOg [4]	✓					9,602	-	-	-
Ref-Reasoning [10]		✓	✓			34,609	-	-	-
Cops-ref [9]		✓			✓	12,586	-	-	37,758
Ref-Adv [6]	✓	✓	✓	✓		9,602	3,704	-	-
Ours	✓	✓	✓	✓	✓	9,605	9,814	8,507	-

III. FINECOPS-REF BENCHMARK

In this section, we provide a detailed description of the FineCops-Ref dataset construction. Our dataset comprises both positive and negative samples. Positive samples consist of paired images and textual expressions, while negative samples contain unpaired images and textual expressions. The negative samples are specifically designed to evaluate the model’s ability to reject instances where the target object is absent from the image. The dataset construction pipeline is illustrated in Fig. 1.

A. Creating Positive Data

Path Generation. We employ image scene graphs from GQA [11] for path generation. The scene graphs contain detailed information about objects, attributes, and relations. To ensure accuracy, we first filter the objects based on their suitability as target or related objects. We leverage annotations from InstInpaint [54] and apply additional filters such as keywords and object size. Next, we generate several paths for each of the filtered objects, as show in Fig. 1(a). To eliminate ambiguity, we utilize unique attributes or relations to identify the target object that shares the same category as other objects in the image to ensure that every generated path is unique.

Data Categorization. We categorize the paths into three difficulty levels based on the complexity of fine-grained reasoning. Level 1 indicates that there are no other objects in the image belonging to the same category as the target object, such as the TV in Fig. 1. In this case, the model can locate the target without requiring contextual understanding. Level 2 signifies the presence of another object with the same category as the target in the image, where the target can be distinguished through one unique attribute or relation. Level 3 requires at least two or more relationships and attribute information. The difficulty levels are determined by the intricacy of fine-grained reasoning, rather than the complexity of the textual description.

Expression Generation. To mitigate potential biases in the scene graphs, we first apply frequency-based sampling of relationships, attributes, and object categories along the generated paths. Subsequently, we use predefined templates to generate referring expressions. The details of predefined templates are provided in Appendix.

To further augment the naturalness and diversity of these expressions, we leverage GPT-3.5-turbo to rewrite the referring

expressions. By incorporating well-designed instructions and examples, we achieve a wider range of linguistically diverse and natural expressions. The prompts used for rewriting are listed in Appendix.

Human Filter. Due to inherent limitations in the scene graph annotations, the generated paths, particularly for Level 2 and Level 3, may contain inaccuracies, leading to non-unique target references. To address this, human annotators manually filtered the test set. Further details can be found in Appendix.

B. Generating Negative Data

To conduct a thorough and systematic assessment of REC of existing VLMs, we generate hard negatives from both textual and visual sources. Similar to positive data, negative data are categorized into different levels based on difficulty. Negative Level 1 involves alterations to the target object in the expressions, which are relatively straightforward for the model to identify. Level 2 involves modifications to the related objects, disrupting the contextual information and posing a greater challenge for existing models to recognize.

Generating Negative Expressions. Our set of negative expressions encompasses a wide range of challenging types. Inspired by CREPE [55] and SUGARCREPE [56], we consider various forms of hard negatives. In total, FineCops-Ref covers 5 fine-grained types of hard negative expressions. These types can be broadly classified into two categories: Replace and Swap. The Replace category involves generating negative expressions by substituting a portion of the original expression, whether it is an object, attribute, or relation. We utilize LLM to determine the most appropriate negative word, ensuring that the negative expression is genuinely negative while only slightly deviating from the original expression. We experimented with various replacement methods and found that LLM-based replacements performed the best, as discussed in Appendix. The Swap category entails generating negative expressions by interchanging two attributes or objects within the same category. We further employ LLM to rewrite these new expressions.

Generating Negative Images. We consider the necessity of negative images from the following aspects. First, negative images enables a more thorough assessment of models’ visual parsing capabilities. Additionally, evaluations conducted by

TABLE II: Dataset statistics.

Set	Positive	Negative expression	Negative image
Train	163,792	80,451	-
Val	18,455	9,029	-
Test	9,605	9,814	8,507

Visualgptscore [57] suggest that negative expressions may lack plausibility and fluency and can be detected by language prior.

We generate hard negative images with subtle differences from the original, such as modifications to objects, attributes, or relations. For simple positional relationships, we employ horizontal flips. For more intricate modifications involving objects and attributes, we utilize PowerPaint [58], an exceptional image inpainting model offering versatility, to perform precise edits on the images. To guide PowerPaint in editing the image, we utilize LLM-generated replacements as textual guides and the bounding boxes as masks. Overall, FineCops-Ref encompasses 5 distinct types of challenging negative images. Further details on the data types, along with example expressions and images, can be found in Appendix.

Negative Data Debiasing. During the generation of negative samples, some implausible or incoherent expressions, as well as unreasonable and easily distinguishable negative images, are inevitable. We employed several techniques to filter out unsuitable samples and improve the quality of the benchmark. For negative expressions, we employ the Adversarial Refinement technique proposed by SUGARCREPE [56], which helps mitigate biases and unintended artifacts in the dataset.

To exclude inappropriate and excessively unreasonable negative images, we employ a multi-step filtering process. First, we use CLIP [59] to ensure that the similarity between the negative text and the positive image is lower than the similarity between the positive text and the positive image. Next, we apply the diffusion-generated inspection model DIRE [60] to filter out excessively unnatural images, excluding those with scores above 0.2. Finally, we use DINOv2 [61] to compute the image-image similarity between the positive image and the generated negative images, retaining the candidate negative image with the highest DINOv2 score from a set of 10 candidates, thereby minimizing noise.

C. Dataset Statistics

FineCops-Ref consists of 9,605 positive expressions, 9,814 negative expressions, and 8,507 negative images in test set. Table I provides a comparison between FineCops-Ref and other visual grounding benchmarks. FineCops-Ref combines the advantages of unconstrained expression, fine-grained compositional reasoning, difficulty level, and hard negatives at both textual and visual levels. Additionally, we partition the training set and validation set simultaneously as in Table II. For more statistics, please refer to the Appendix.

D. Metrics

To evaluate performance on positive data, we use the common metric Precision@k. When both positive and negative

data are present in the test set, we treat the negative samples as distractors for the positive samples, and introduce two additional metrics:

Recall@k: We treat the REC task as a bounding box retrieval problem. For each negative sample paired with its corresponding positive sample, we first obtain the predicted bounding boxes from the model, along with their confidence scores for both positive and negative samples. These bounding boxes are then ranked based on their confidence scores. Recall@k measures the proportion of negative-positive pairs where at least one of the top k predicted bounding boxes has an IoU greater than 0.5 with the ground truth bounding box. It specifically assesses the model’s ability to avoid assigning high confidence scores to negative samples. Formally, Recall@k is defined as:

$$\text{Recall@k} = \frac{1}{N} \sum_{i=1}^N \mathbb{1} \left(\max_{j \in \{1, \dots, k\}} \text{IoU}_{i,j} > 0.5 \right), \quad (1)$$

where N represents the total number of negative-positive pairs, and $\mathbb{1}(\cdot)$ is an indicator function that equals 1 if the condition inside is true and 0 otherwise. The term $\text{IoU}_{i,j}$ refers to the overlap between the j -th predicted bounding box (ranked based on the confidence scores) and the ground truth bounding box for the i -th pair. Note that for negative samples, there is no ground truth box, meaning the IoU is 0.

Recall@k is commonly used in retrieval tasks to assess prediction accuracy in the presence of challenging negative samples. Ideally, the model should assign lower confidence scores to negative samples. In our study, we primarily report Recall@1. If the model consistently assigns lower confidence scores to negative samples compared to positive ones, Recall@1 should equal Precision@1.

AUROC: While Recall@k evaluates how well the model ranks individual negative samples relative to their corresponding positive samples, it does not offer a holistic view of confidence across the dataset. To address this, we use AUROC to measure the overall ability of the model to distinguish between positive and negative samples. AUROC measures the model’s ability to correctly rank positive samples higher than negative ones across the datasets, providing a holistic view of its discriminative power.

By combining Recall@k and AUROC, we ensure a comprehensive evaluation of the model’s performance in distinguishing between positive and negative samples in REC tasks. This dual approach addresses both specific ranking and overall confidence.

IV. METHOD

Referring Expression Comprehension presents a unique challenge in computer vision, demanding not only precise object detection but also compositional visual reasoning to ground natural language descriptions to specific image regions. Specialist Models, such as MDETR [29] and Grounding DINO [62], demonstrate efficiency and excel at accurate object detection and grounding. Their strengths lie in their optimized architectures and training on extensive datasets with bounding box annotations, enabling precise box regression and

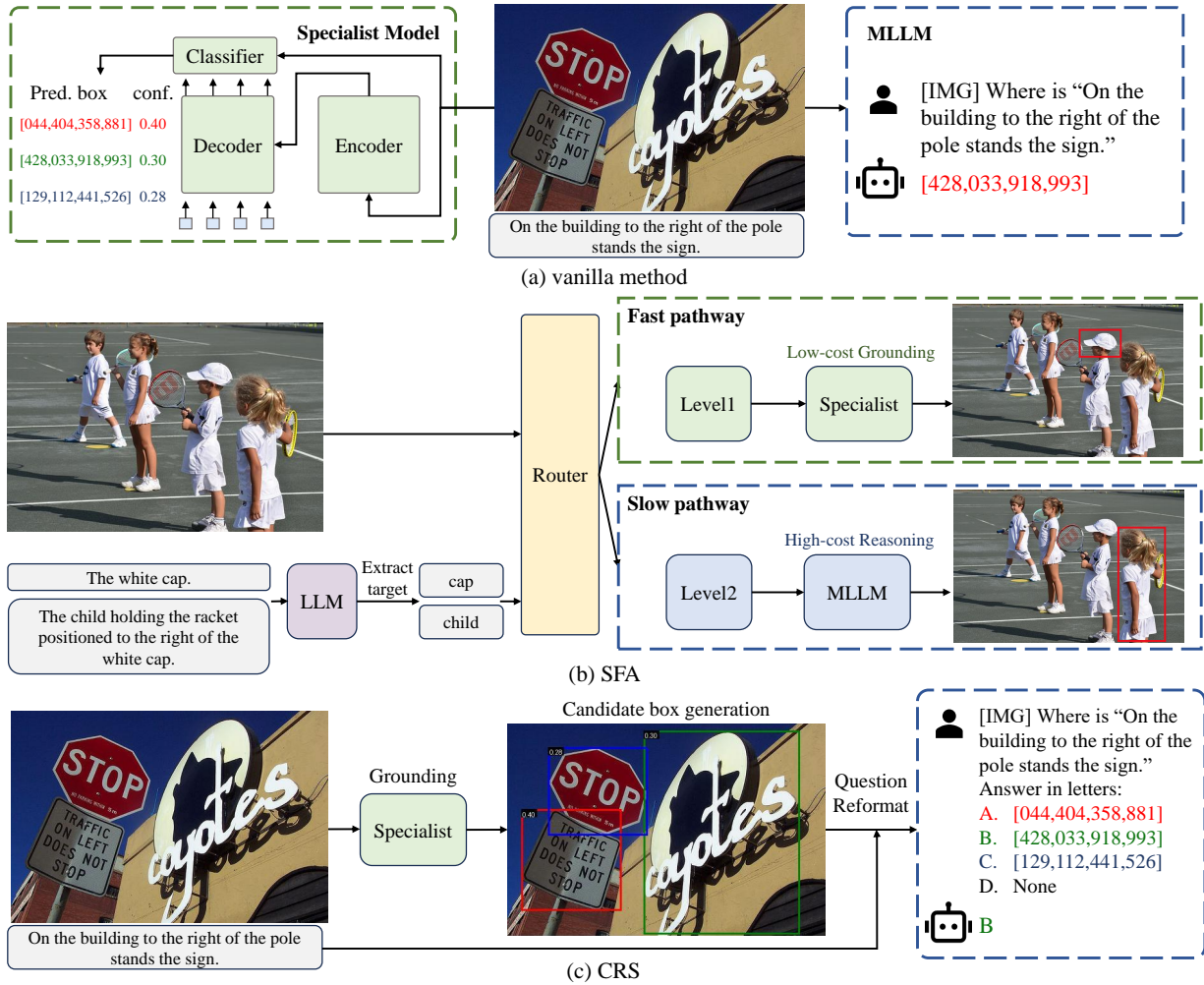


Fig. 2: (a) Vanilla Model: The Specialist Model uses box regression to output multiple candidate boxes with confidence scores and selects the region with the highest confidence. In contrast, MLLMs directly generate object coordinates as text. (b) Slow-Fast Adaptation (SFA): A router categorizes tasks by complexity (Level 1/2). Level 1 tasks are processed using the fast pathway (Specialist Model), while Level 2 tasks are processed using the slow pathway (MLLM). (c) Candidate Region Selection (CRS): The Specialist Model generates multiple candidate bounding boxes, and the MLLM selects the best option in a multi-choice selection task.

rapid processing. These models deliver exceptional grounding accuracy and high Recall@k, ensuring that the correct object is often among the top predictions. Indeed, for simpler REC instances where target identification relies primarily on object category, Specialist Models often suffice. However, Specialist Models exhibit limitations in handling the inherent complexity of natural language. They often struggle with referring expressions that require compositional reasoning, disambiguation among multiple objects of the same category.

In contrast, MLLMs exhibit strong reasoning capabilities, making them well-suited for complex REC tasks that require deeper semantic understanding. However, they are computationally demanding and not inherently optimized for grounding tasks, as they generate bounding box coordinates directly as part of a text generation process, rather than leveraging intermediate bounding box proposals as informative priors, as specialist models do.

This motivates our collaborative approach, which aims to

synergistically combine the strengths of Specialist Models and MLLMs while mitigating their respective weaknesses. We recognize the complementary nature of these architectures: Specialist Models offer efficiency and strong grounding capabilities, particularly valuable for precise object localization and candidate generation, while MLLMs provide the crucial reasoning abilities needed for disambiguation and complex expression understanding. By strategically integrating these model types, we can achieve superior REC performance with improved computational efficiency compared to relying solely on resource-intensive MLLMs.

Motivated by this insight, we introduce two novel strategies: **Slow-Fast Adaptation (SFA)** and **Candidate Region Selection (CRS)**. SFA routes REC tasks based on their inherent complexity. Simpler tasks, where Specialist Models are adept, are processed efficiently, while more complex tasks requiring reasoning are directed to MLLMs. This dynamic routing optimizes overall computational cost without sacrific-

ing performance. **CRS** leverages the strong object detection of Specialist Models to generate a set of candidate regions, and then employs an MLLM to reason over these candidates and select the most appropriate one. The subsequent subsections detail each method, elucidating their specific mechanisms and implementation.

A. Slow-Fast Adaptation (SFA)

The Slow-Fast Adaptation (SFA) strategy is designed to optimize both performance and computational efficiency in a training-free manner. As illustrated in Fig. 2(b), SFA operates by utilizing a router to evaluate task complexity and directing tasks to either a fast or slow pathway based on their difficulty level. Given an image and a referring expression, the process begins with target extraction and difficulty level assessment, followed by task routing to the appropriate pathway.

Target Extraction. Given a referring expression, we employ GPT-3.5-turbo to extract the target object by prompting: “Which object does the given expression refer to?”. To minimize hallucinations by GPT, we include three in-context examples in the prompt and require GPT to respond in dictionary format. Detailed prompts are provided in the supplementary material.

Difficulty Level Assessment. We categorize REC tasks into two levels based on the presence of distracting objects in the image:

- Level 1: The image contains single instance of the referred object, which can be easily identified based on the category name (e.g., a single white cap in the image, as shown in Fig. 2(b)).
- Level 2: The image contains multiple instances of the target category, requiring compositional reasoning to disambiguate the correct target (e.g., identifying a child “positioned to the right of the white cap” among several children, as shown in Fig. 2(b)).

To assess task complexity, we employ a low-cost routing method: object detection is performed on the extracted target category using MM-GDINO-L [62] with a confidence threshold of 0.2. The number of detected objects above this threshold determines the task’s difficulty level. If only one object is detected, the task is classified as Level 1; otherwise, it is

classified as Level 2. This approach ensures efficient routing while minimizing computational overhead.

Task Routing. Based on the difficulty level, tasks are routed to one of two pathways: Simple tasks are processed using low-cost Specialist Models (e.g., Grounding DINO), which make quick judgments based on the target object’s category. On the other hand, complex tasks are processed using resource-intensive MLLMs, which leverage their superior reasoning capabilities to disambiguate the target object through compositional reasoning.

Notably, the SFA strategy does not require additional training and introduces minimal computational overhead. By dynamically routing tasks based on their complexity, SFA effectively combines the efficiency of Specialist Models with the reasoning ability of MLLMs, achieving higher performance while maintaining computational efficiency.

Focus-enhancement Strategy. In our work, we observe that models often struggle to correctly identify the target object category referred to in an expression, frequently detecting instances from other categories mentioned in the description instead. To mitigate this issue, we propose a focus-enhancement strategy—a simple yet effective method that encourages models to precisely concentrate on the intended target category derived from the referring expression.

Target-focus Matching for Specialist Models. Fig. 3 illustrates the focus-enhancement strategy for Specialist Models, specifically the target-focus matching mechanism. By default, MM-GDINO [62] computes similarity scores between image tokens and all textual tokens, selecting the proposal with the highest overall score as the output. In contrast, our method refines this process by focusing solely on the similarity scores associated with the target extracted from the referring expression, ensuring that the proposal with the highest target-specific score is selected. This approach proves effective, as cross-modal feature fusion enables the target-specific token to capture both the full semantic context of the expression and the corresponding visual context. By leveraging context-aware, target-specific textual features for matching, our method filters out distracting information while preserving the essential meaning of the expression, thereby improving accuracy. As shown in Fig. 3, by restricting selection to scores associated with the term “bird,” our method avoids incorrect

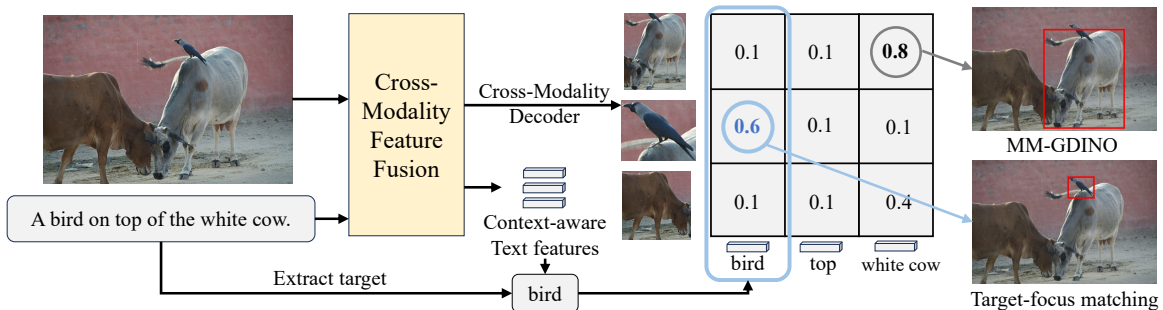


Fig. 3: Illustration of the target-focus matching for Specialist Models. The target is extracted from the referring expression using a LLM. Leveraging the cross-attention mechanism, the target’s feature becomes context-aware, enabling more accurate matching with the proposal. This approach helps avoid mismatches with other objects mentioned in the expression, an issue observed in the original solution (e.g., MM-GDINO [62]).

matches (e.g., where the score for “white cow” is higher) and accurately identifies the intended target.

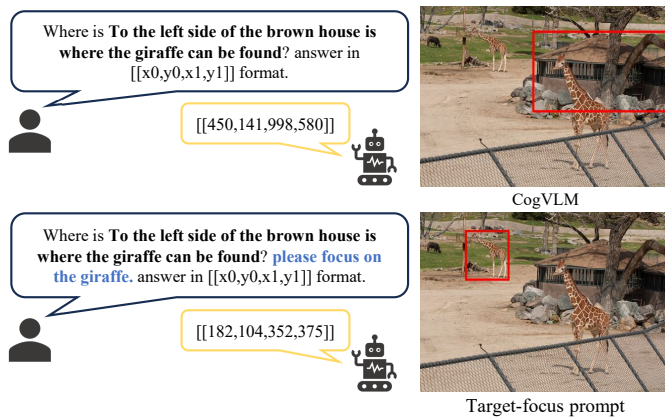


Fig. 4: Target-focus prompt for MLLMs. The default prompt used by CogVLM [43] is “Where is $\langle \text{expr} \rangle$? answer in $[[x_0, y_0, x_1, y_1]]$ format.” as shown above. To enhance focus, we modify the prompt by appending “please focus on the $\langle \text{target} \rangle$ ”, where $\langle \text{target} \rangle$ donates the target extracted by LLM from the textual expression.

Target-focus Prompt for MLLMs. Fig. 4 illustrates the focus-enhancement strategy for MLLMs, specifically the target-focus prompt. We add a simple prompt like “please focus on the $\langle \text{target} \rangle$ ”, where $\langle \text{target} \rangle$ denotes the extracted target from the expression. As shown in Fig. 4, without the target-focus prompt, CogVLM [43] incorrectly identifies the target as “house”. However, after incorporating the target-focus prompt, the model correctly understands the intended reference “giraffe” and accurately locates its instance on the left side of the image. The purpose of this enhanced prompt is to explicitly emphasize the target of interest within the expression, guiding the model toward more precise interpretation and localization.

B. Candidate Region Selection (CRS)

The Candidate Region Selection (CRS) strategy combines the complementary strengths of Specialist Models and MLLMs in a cost-effective manner. In standard REC tasks, Specialist Models output bounding boxes and typically select the highest-confidence one as the target. However, this approach can fail when the correct target is not the highest-confidence box or when multiple objects from the same category are present. By exploring the top-k bounding boxes, CRS expands the candidate set, improving the likelihood of selecting the correct target in ambiguous cases. Integrating an MLLM allows for effective disambiguation, enabling the model to reason over the top-k candidates and select the correct one through a multiple-choice format.

CRS Pipeline. As shown in Fig. 2(c), the CRS strategy begins by applying a Specialist Model (e.g., Grounding DINO) for object detection, generating a set of candidate bounding boxes. Non-Maximum Suppression (NMS) with a 0.7 threshold is then applied to remove redundant predictions. From the remaining boxes, the top-k highest-confidence ones are selected as potential targets.

These candidates are passed to the MLLM, which processes them in a multiple-choice format. The MLLM selects the correct bounding box by outputting a single token (e.g., “A”), simplifying the prediction process compared to traditional autoregressive methods that predict bounding box coordinates sequentially. This approach not only reduces inference time but also provides the MLLM with more prior information for accurate target detection.

Instruction Tuning for Multi-Choice Region Selection. While MLLMs are effective for cross-modality reasoning, which is crucial for REC, they may not perform well in the multi-choice region selection task. This is because they were not originally trained for this specific multiple-choice format. To address this, we propose instruction tuning tailored for multi-choice region selection. However, directly tuning the MLLM on the target dataset risks information leakage. Instead, we suggest that the MLLM only needs to acquire the ability to perform region selection, so we construct the instruction tuning dataset based on the external RefCOCO series, a standard REC benchmark that most MLLMs have already encountered during training.

Specifically, we generate a set of top-k bounding boxes for each referring expression using Grounding DINO and retain only those samples where the correct prediction (IoU > 0.5) is within the top-k predictions. These are then shuffled to create candidate choices. This approach allows the MLLM to learn to distinguish between plausible bounding boxes and refine its ability to select the correct one based on both visual and linguistic context.

This instruction tuning strategy equips the MLLM to better handle the multiple-choice format, improving its region selection accuracy while maintaining computational efficiency.

Multi-Choice Instruction Tuning with None Option. A key limitation of MLLMs is their difficulty in rejecting inappropriate queries, largely due to the lack of negative samples in the training data and well-defined refusal mechanisms. To address this, we propose an enhanced instruction tuning approach, sampling 10,000 positive and 2,500 negative samples from the FineCops-ref training set.

Expanding on the standard multiple-choice formulation, we introduce an additional “None” option (e.g., “D. None”) to represent cases where no valid target exists. Our experimental results show that this approach significantly improves the model’s ability to reject negative samples while maintaining high accuracy on positive samples.

V. EXPERIMENTS

In this section, we present the experimental results. In subsection V-A, we benchmark FineCops-Ref dataset by evaluating various representative models. The evaluation focuses on the models’ ability to accurately localize the target and reject non-existent objects. In Subsection V-B, we assess the effectiveness of the proposed Specialist-MLLM collaboration approaches—namely, Slow-Fast Adaptation (SFA) and Candidate Region Selection (CRS)—through comparisons with existing state-of-the-art (SOTA) methods. Finally, in Subsection V-C, we provide the results of ablation studies to further validate our approach.

TABLE III: Evaluation results (Precision@1) on positive data. L1, L2, and L3 represent Level1, Level2, and Level3 of the ground truth labels in FineCops-Ref, respectively. The best results are in bold, and the second-best results are underlined.

Model	Positive			
	L1	L2	L3	All
Specialist				
UNINEXT [30]	59.95	43.60	40.98	53.22
SimVG [38]	61.88	47.30	42.04	55.74
MM-GDINO-T [62]	75.11	34.78	35.46	58.87
MDETR [29]	73.25	53.08	46.71	64.80
MM-GDINO-L [62]	85.13	43.54	42.89	68.32
MLLM				
GPT4-V [63] + SoM [46]	55.94	45.94	49.29	52.07
Shikra [39]	64.64	50.29	43.95	58.54
Lenna [42]	73.75	41.92	38.43	60.74
GroundingGPT [41]	71.10	53.64	49.89	63.87
Ferret-13B [40]	70.24	55.99	50.53	64.23
InternVL2.5-8B [53]	70.91	59.67	53.08	66.05
CogVLM [43]	74.59	<u>62.51</u>	57.32	69.46
CogCom [44]	76.27	<u>60.93</u>	<u>59.87</u>	<u>70.03</u>
Qwen2-VL-7B [52]	<u>78.24</u>	66.13	60.72	73.09

A. Benchmarking the FineCops-Ref Dataset

1) **Evaluated Models:** We evaluate several representative models, including both Specialist Models and MLLMs. The models examined in this study include UNINEXT [30], SimVG [38], MDETR [29], MM-GDINO [31], [62], Shikra [39], Ferret [40], GroundingGPT [41], Lenna [42], CogVLM [43], CogCom [44], InternVL2.5 [53] and Qwen2-vl [52]. We use their open-source checkpoints for evaluation. Additionally, we evaluate GPT4-V [63], which has limited capability in directly outputting bounding boxes. To assess its performance, we combine GPT4-V with the Set-of-Mark (SoM) [46]. Details on the model source and implementation are provided in the Appendix.

2) **Evaluation on Positive Data:** We evaluate the models using Precision@1 for positive data, as summarized in Table III. The results highlight the importance of categorizing the dataset by difficulty levels, as the performance of most models degrades significantly with increasing complexity. Notably, at difficulty level 3, the majority of models achieve a precision below 50%. An interesting observation is that models like UNINEXT, SimVG, and InternVL2.5, which achieve state-of-the-art performance on the RefCOCO series benchmarks, perform relatively poorly on the FineCops-Ref benchmark. In contrast, Grounding DINO and Qwen2-VL demonstrate strong generalization capabilities, achieving the best results in the Specialist and MLLM categories, respectively.

Specialist performs better on simple REC tasks. At Level 1, the task primarily involves identifying objects based on category names, closely aligning with the requirements of open-vocabulary object detection. Grounding DINO, built on the SWIN-L backbone, achieves an impressive accuracy of 85.13% under this settings. This observation leads to two key insights. First, vision-language models focused on object detection exhibit strong capabilities in basic visual localization

and object detection tasks, even in zero-shot scenarios, which is also supported by their superior performance on RefCOCO benchmark which mainly require the model to detect the object without consider the intricate attribute and relation. Second, although MLLMs excel in language understanding and reasoning, their basic object detection abilities still fall short of the standards required for truly general-purpose models.

MLLMs exhibit superior reasoning abilities. At Level 2 and 3, the tasks demand sophisticated language understanding and cross-modal reasoning due to the presence of numerous easily confusable objects in the images. However, most models do not exhibit sufficient capability in this regard. MLLMs based on large language models (LLMs) perform better in this aspect, showcasing their superior compositional reasoning abilities.

3) **Evaluation on Negative Data:** We evaluate the models using Recall@1 and AUROC for negative data. The AUROC results can be found in Appendix. Specifically, models like MDETR and Lenna that have dedicated object detection modules can generate multiple detection boxes with associated confidence scores, allowing for direct computation of Recall@1 and AUROC. For models that generate coordinates as text using an autoregressive approach, we use the probability of the coordinate tokens to calculate confidence [14], [64]. The evaluation results for negative expressions and negative images are shown in Table IV and Table V, respectively. The results indicate that existing models generally exhibit low recall@1 performance on negative data, with most values falling below 50%. This suggests that these models have weak rejection capability for non-existent objects. In contrast, the latest model, Qwen2-VL, demonstrates strong generalization ability and achieves the best performance. According to the experimental results, we can draw the following conclusions:

The models struggle with compositional reasoning and exhibit a limited understanding of semantic structures. L1 and L2 represent two levels of modification: L1 refers to direct changes related to the target, including objects, attributes, and relations, while L2 involves changing other object-related elements, which are often more challenging to detect. For the same type of negative data, the recall of L1 is typically significantly higher than that of L2, suggesting that most models can effectively identify simple anomalies, such as changes directly related to the target. However, for L2 negative data, almost all models perform poorly. This further highlights that the models lack compositional reasoning ability and fail to fully comprehend the semantic structure of sentences.

The models exhibit poor understanding of fine-grained attributes and relations. For negative data at the same level, the recall of changing attributes is generally lower than that of changing objects, while the recall of changing relations is typically significantly lower than the first two. This suggests that the models exhibit relatively stronger object recognition capabilities but weaker understanding of attributes and relations. Specifically, the models perform poorly on negative data involving the “replace relation” and “flip” types, indicating substantial challenges in relation comprehension. Another notable observation is that, compared to directly replacing attributes, the models perform worse when identifying negative

TABLE IV: Evaluation results (Recall@1) on negative expressions. L1 and L2 denote the direct changes related to the target and the changes related to other objects within the expression, respectively.

Model	REPLACE						SWAP				Avg.
	Object		Attribute		Relation		Object		Attribute		
	L1	L2									
Specialist											
MM-GDINO-T [62]	58.84	33.77	50.47	29.96	34.69	31.92	43.89	27.71	43.67	31.97	38.69
UNINEXT [30]	47.83	33.70	44.66	34.30	39.51	35.61	45.31	37.35	41.69	31.97	39.19
MDETR [29]	52.89	36.09	50.47	35.92	42.48	40.77	45.89	37.35	44.42	37.70	42.40
SimVG [38]	43.45	43.20	46.46	44.04	40.33	45.20	41.00	31.93	40.20	50.82	42.66
MM-GDINO-L [62]	<u>64.23</u>	40.26	55.76	41.52	45.74	43.73	53.02	<u>48.19</u>	<u>49.38</u>	37.70	47.95
MLLM											
Ferret-13B [40]	38.38	33.01	37.57	34.48	35.58	34.69	38.69	34.94	35.73	35.25	35.83
GroundingGPT [41]	42.24	35.13	40.14	33.75	37.51	36.72	41.77	39.76	35.24	39.34	38.16
Shikra [39]	44.99	33.11	41.25	33.03	35.78	39.85	42.27	39.16	39.70	32.79	38.19
InternVL2.5-8B [53]	38.55	36.16	41.84	37.91	40.92	39.48	39.40	39.16	43.92	38.52	39.58
CogVLM [43]	53.34	44.02	51.24	48.74	41.22	<u>44.46</u>	47.69	49.40	46.40	40.16	46.67
CogCom [44]	57.96	44.91	54.65	44.04	45.81	41.70	<u>51.03</u>	43.98	47.39	36.89	46.84
Lenna [42]	65.88	50.38	58.75	42.96	47.00	43.91	49.94	38.55	<u>49.38</u>	43.44	49.02
Qwen2-VL-7B [52]	60.63	<u>45.62</u>	59.59	<u>46.93</u>	49.18	42.44	49.13	46.99	50.87	<u>44.26</u>	49.56

TABLE V: Evaluation results (Recall@1) on negative images.

Model	REPLACE				SWAP					Avg.
	Object		Attribute		Object	Attribute		Flip		
	L1	L2	L1	L2	L1	L1	L2	L1	L2	
Specialist										
UNINEXT [30]	48.85	31.62	40.96	30.33	46.91	40.25	37.06	30.66	29.42	37.34
SimVG [38]	41.69	41.50	43.73	43.15	31.60	38.60	<u>51.75</u>	36.74	39.66	40.94
MM-GDINO-T [62]	58.46	40.73	44.75	37.61	46.25	51.33	28.67	39.50	40.94	43.14
MDETR [29]	58.15	42.85	51.70	37.95	48.86	49.49	44.76	44.29	42.22	46.70
MM-GDINO-L [62]	66.35	49.45	<u>54.93</u>	<u>49.05</u>	<u>55.05</u>	62.63	46.85	<u>45.21</u>	<u>46.48</u>	<u>52.89</u>
MLLM										
CogCom [44]	32.24	21.55	22.57	20.10	39.74	25.46	18.88	24.13	23.03	25.30
Shikra [39]	42.57	33.61	36.54	34.26	35.18	38.60	36.36	34.25	37.10	36.50
GroundingGPT [41]	43.91	36.88	36.31	35.88	39.09	37.17	40.56	37.02	33.05	37.76
Ferret-13B [40]	41.54	37.46	38.04	36.22	43.00	37.78	39.16	35.27	36.25	38.30
InternVL2.5-8B [53]	42.96	41.57	39.46	40.80	45.93	44.35	45.45	42.08	40.72	42.59
Lenna [42]	<u>66.88</u>	<u>51.19</u>	54.38	39.34	47.56	49.08	43.36	33.98	30.92	46.30
CogVLM [43]	51.11	49.01	43.49	46.10	50.49	<u>53.80</u>	49.65	43.74	37.74	47.24
Qwen2-VL-7B [52]	69.73	60.65	63.87	58.41	63.52	62.63	54.55	61.88	52.45	60.85

data of the “swap attribute” type, highlighting their limitations in accurately associating attributes.

B. Evaluation of the Proposed Specialist-MLLM Collaboration Approaches

In this section, we compare our proposed Specialist-MLLM collaboration methods with representative REC models, including both Specialist Models and MLLMs. We evaluate the performance using Precision@1. The details for CRS training are provided in Appendix.

1) *Evaluation of Slow-Fast Adaptation (SFA)*: As shown in Table VI, Specialist Models generally perform well on Level 1 tasks, where text-to-region feature matching is essential, while MLLM solutions tend to excel in Level 2 tasks, which require more complex reasoning. This observation supports our task-adaptive model selection strategy. Our SFA approach, which combines the strengths of both methods through effective task routing, achieves superior performance compared to using these strategies individually. Incorporating the focus-enhancement strategy further boosts performance,

with our SFA† yielding additional improvements. These results demonstrate the effectiveness of our solution in handling REC tasks with varying levels of difficulty, highlighting the broad applicability of our approach.

Importantly, thanks to task-specific model selection, our method achieves high efficiency compared to relying solely on MLLMs. As illustrated in Fig. 5(a), our approach outperforms CogVLM [43] by an absolute 5.6% while using only 62% of the computational cost. When compared to Ferret [40], which maintains similar computational overhead, our method achieves over a 10% performance boost. These results demonstrate that our method strikes an optimal balance between performance and efficiency.

Effectiveness of Target-refocus Strategy. To evaluate the generalizability of our proposed focus-enhancement strategy, we apply it to various Specialist and MLLM methods, as shown in Table VII. This strategy helps models focus on the referred target, thereby reducing the misidentification of the target object as another category. The experimental results show that our focus-enhancement strategy consistently improves the performance of both Specialist and MLLM methods

TABLE VI: Comparison with state-of-the-art Specialist and MLLM methods on three REC benchmarks. L1 and L2 denote Level 1 and Level 2, respectively, as determined by the router Grounding DINO [62] in SFA. † indicates the use of the focus-enhancement strategy in our SFA method.

Method	FineCops-Ref			Ref-Adv			Ref-Reasoning		
	L1	L2	All	L1	L2	All	L1	L2	All
Specialist									
UNINEXT	65.39	39.06	53.22	82.55	69.68	75.59	35.03	16.66	20.80
SimVG	66.86	42.80	55.74	82.90	69.83	75.84	35.79	18.64	22.50
MDETR	74.85	53.10	64.80	81.20	67.38	73.73	46.53	26.62	31.10
MM-GDINO-L	81.20	53.32	68.32	85.37	66.08	74.95	50.94	27.09	32.46
MLLM									
Shikra	66.92	48.79	58.54	79.64	66.62	72.31	40.85	23.83	27.18
GroundingGPT	75.38	50.48	63.87	80.20	66.68	72.89	43.30	21.69	26.55
Ferret-13B	73.77	53.12	64.23	81.61	71.73	76.27	42.27	23.23	27.51
InternVL2.5-8B	76.05	54.40	66.05	80.85	71.73	75.92	44.44	25.97	30.13
CogVLM	73.58	64.68	69.46	79.14	71.98	75.27	45.67	33.10	35.93
CogCom	77.89	60.87	70.03	82.20	71.23	76.27	47.29	28.44	32.68
Qwen2-VL-7B	79.40	65.74	73.09	85.84	74.73	79.83	50.62	31.46	35.77
SFA									
CogVLM(SFA)	81.20	64.68	73.57(+4.11)	85.37	71.98	78.13(+2.86)	50.94	33.10	37.11(+1.18)
CogVLM(SFA†)	83.43	65.69	75.03(+5.57)	85.37	72.98	78.37(+3.10)	52.34	34.37	38.41(+2.48)
Qwen2-VL-7B(SFA)	81.20	65.74	74.06(+0.97)	85.37	74.73	79.62(-0.21)	50.94	31.46	35.84(+0.07)
Qwen2-VL-7B(SFA†)	83.43	66.91	75.61(+2.52)	84.78	75.92	79.97(+0.14)	52.34	31.72	36.36(+0.59)
CRS									
CogVLM(CRS)	79.13	67.20	73.62(+4.16)	81.37	74.58	77.70(+2.43)	51.27	33.97	37.87(+1.94)
Qwen2-VL-7B(CRS)	84.77	70.85	78.33(+5.24)	84.37	77.32	80.56(+0.73)	54.80	36.28	40.45(+4.68)
InternVL2.5-8B(CRS)	86.06	69.88	78.58(+12.53)	87.96	78.42	82.80(+6.88)	55.10	36.05	40.34(+10.21)

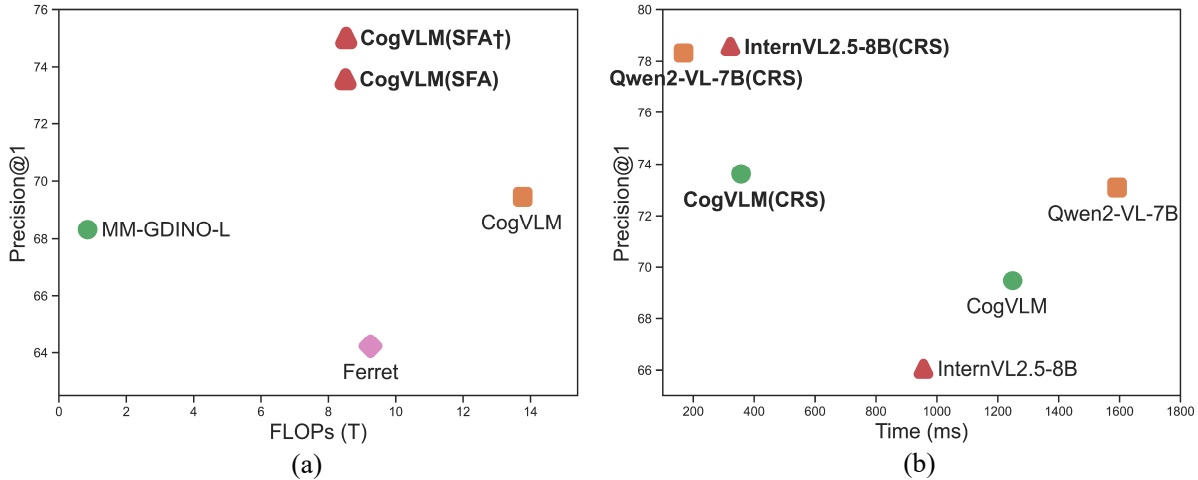


Fig. 5: The effectiveness of the proposed methods. (a) compares the FLOPs (computational cost) of SFA with other methods, including the Specialist Model MM-GDINO-L [62] and MLLMs such as CogVLM [43] and Ferret [40]. (b) compares the inference time of CRS with that of MLLMs themselves.

across all datasets, demonstrating its effectiveness and broad applicability.

2) *Evaluation of Candidate Region Selection (CRS)*: As shown in Table VI, our CRS method consistently achieves improvements across all three benchmarks. Notably, when applied to InternVL2.5 [53], CRS delivers a remarkable performance boost of nearly 10%. The experimental results demonstrate that advanced models possess substantial cross-modal reasoning capability. Through instruction tuning, we effectively harness these inherent capabilities, enabling the model to achieve stronger grounding performance and fully

unleash its potential. These findings underscore both the effectiveness and generalizability of our approach.

It is important to note that, while CRS slightly increases the length of input tokens, it significantly reduces the length of output tokens (from n to 1). In practical applications, this reduction leads to a considerable improvement in inference speed. As illustrated in Fig. 5(b), CRS requires only 10%-30% of the inference time compared to the original method, underscoring the strong practical value of our approach.

As shown in Fig. 6, both Grounding DINO and InternVL2.5 output wrong bounding boxes. However, after applying the

TABLE VII: Effectiveness of the proposed focus-enhancement strategy. *Exp.* denotes the original method, *Foc.* indicates our focus-enhancement strategy, which can be readily applied to various Specialist and MLLM methods.

Model	Method	FineCops-Ref	Ref-Adv	Ref-Reasoning
Specialist				
MDETR [29]	Exp.	64.80	73.73	31.10
	Foc.	67.19(+2.39)	72.12(-1.61)	34.65(+3.55)
MM-GDINO-L [62]	Exp.	68.32	74.95	32.46
	Foc.	71.22(+2.90)	74.55(-0.40)	34.28(+1.82)
MLLM				
GroundingGPT [41]	Exp.	63.87	72.89	26.55
	Foc.	65.90(+2.03)	74.33(+1.44)	28.11(+1.56)
Ferret-13B [40]	Exp.	64.23	76.27	27.51
	Foc.	66.10(+1.87)	78.07(+1.80)	28.96(+1.45)
CogVLM [43]	Exp.	69.46	75.27	35.93
	Foc.	72.11(+2.65)	77.75(+2.48)	37.12(+1.19)
InternVL2.5-8B [53]	Exp.	66.05	75.92	30.13
	Foc.	69.89(+3.84)	80.29(+4.37)	32.29(+2.16)
Qwen2-VL-7B [52]	Exp.	73.09	79.83	35.77
	Foc.	75.03(+1.94)	80.89(+1.06)	36.16(+0.39)

CRS method, InternVL2.5, leveraging the candidate boxes provided by Grounding DINO and effectively comprehending the relationship in the expression, successfully selects the correct answer: “B”.

TABLE VIII: Evaluation of CRS effectiveness in non-existent target rejection across three settings: (1) CRS without instruction tuning (w/o instruction tuning); (2) instruction tuning with the original prompt (baseline); and (3) instruction tuning with the CRS prompt (CRS).

Finetune	Model	Accuracy		Recall	
		positive	negative	text	image
w/o instruction tuning	InternVL2.5-8B	73.24	11.80	54.91	54.69
	Qwen2-VL-7B	74.50	5.20	55.37	56.59
Baseline	CogVLM	67.83	0.99	45.76	45.84
	Internvl2.5-8B	69.90	58.32	55.06	56.00
	Qwen2vl-7B	64.45	62.31	55.30	54.97
CRS	CogVLM	70.57	36.52	53.65	55.48
	InternVL2.5-8B	76.74	58.63	69.54	68.31
	Qwen2-VL-7B	79.00	27.08	64.98	68.16

Another advantage of our CRS strategy is its inherent ability to reject non-existent objects by selecting a “None” option. To evaluate this capability, we assess three approaches: (1) using the CRS method without instruction tuning (w/o instruction tuning); (2) instruction tuning an MLLM model with its original REC prompt, followed by the instruction “If no target object exists, please output “None” (Baseline); and (3) instruction tuning the model using the CRS prompt, followed by the instruction “If no suitable option exists, please select the option corresponding to “None” (CRS). We evaluate the models using Accuracy and Recall@1, as summarized in Table VIII. For positive data, Accuracy is equivalent to Precision@1, while for negative data, Accuracy measures the proportion of negative data for which the model correctly selects the “None” option. Recall@1 reflects the average recall score.

The experimental results indicate that, without instruction

The long snowboard, can be found resting to the right of the pair of skis.

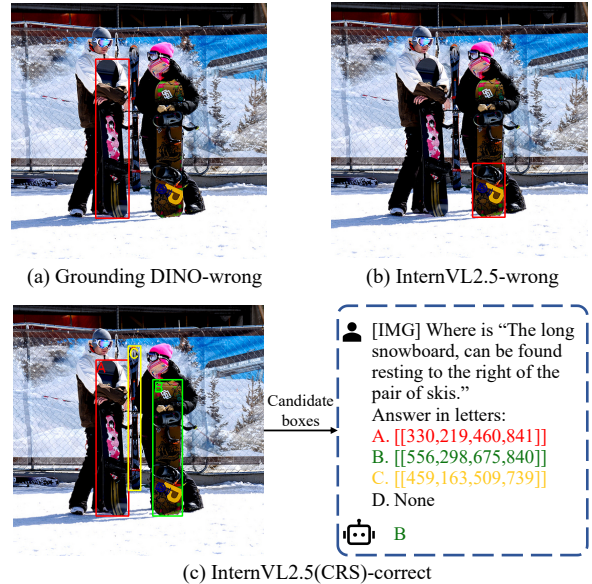


Fig. 6: Visualization of grounding results for Grounding DINO [62], InternVL2.5 [53], and the CRS approach.

tuning, models frequently fail to select “None,” suggesting that existing models have limited rejection capabilities for non-existent objects. This observation aligns with our previous conclusions. After instruction tuning with the baseline method, models manage to respond with “None,” but their accuracy on positive data drops significantly. This indicates that models fail to properly learn when they should reject. In contrast, instruction tuning with the CRS method improves accuracy on both positive and negative data and demonstrates a substantial advantage in Recall@1. These results validate the effectiveness of the CRS method: the models successfully learn to reject non-existent objects while maintaining precise localization performance for positive data.

C. Ablation Studies

In this section, we present extensive ablation studies on our proposed methods. For SFA, we analyze the impact of different detection-based difficulty-level assessment methods on performance. For CRS, we explore various training configurations, including dataset selection and the number of candidates used for region selection.

1) *Ablation on Difficulty-level Assessment Methods in SFA:* In SFA, we use an object-detection based strategy to assess task difficulty, which then guides model selection. Specifically, we extract instances that belong to the target category and check if there are multiple instances of that category. To evaluate this approach, we test different object detection methods, selected based on both inference time and detection capacity. The models we choose need to support open vocabulary detection due to the open-world nature of general target extraction.

We compare difficulty-level recognition accuracy and Level 2 recall on FineCops-Ref, which provides ground-truth difficulty-level labels. As shown in Table IX, Ground-

TABLE IX: Ablation study of different detection-based difficulty-level assessment methods. Difficulty-level assessment accuracy and L2 recall are evaluated on the FineCops-Ref benchmark, based on ground-truth labels provided.

Method	Accuracy	L2 Recall	FineCops-Ref	Ref-Adv	Ref-Reasoning	Time (ms)
OV-DINO [65]	58.46	34.99	70.39	77.11	35.32	112
ProxyDet [66]	57.82	46.53	70.97	78.21	34.76	79
YOLO-World [67]	67.35	28.70	71.53	77.81	34.15	44
MDETR [29]	61.64	63.34	72.72	79.29	36.18	26
MM-GDINO-L [62]	66.75	66.06	74.06	79.62	37.11	381

ing DINO [62] achieves superior performance due to its stronger vision backbones. Accuracy indicates the precision of difficulty-level assessment, reflecting the rationality of task complexity division. Level 2 recall measures the proportion of ground-truth Level 2 tasks correctly identified. A higher Level 2 recall suggests that more complex tasks are appropriately assigned to MLLMs. While considering accuracy, it’s crucial to maintain a high Level 2 recall because Specialist Models handle complex tasks poorly, and misassigning these tasks to Specialist Models can significantly degrade SFA performance. Therefore, we select MM-GDINO-L [62] as our detection method, despite its higher computational cost, which remains within acceptable limits.

TABLE X: Ablation study of variation in dataset and dataset sizes in instruction tuning for CRS. † denotes the use of multi-choice instruction tuning.

Model	Data source	Data size	FineCops-Ref	Ref-Adv	Ref-Reasoning
Qwen2-VL-7B [52]	-	-	73.09	79.83	35.77
Qwen2-VL-7B†	RefCOCO+/g	2k	74.95	76.40	38.88
		4k	76.49	77.94	39.54
		6k	77.67	79.43	39.93
		8k	78.25	80.37	40.35
		10k	78.33	80.56	40.45
		12k	78.84	81.32	40.68
	FineCops-Ref	10k	81.38	82.64	42.05

2) *Ablation on Dataset Variation in Instruction Tuning for CRS:* In the CRS approach, we construct datasets from RefCOCO+/g [2]–[4] to perform multi-choice instruction tuning. This strategy prevents test data leakage and helps the model adapt to the new output format. Table X shows that performance improves consistently as the dataset size increases from 2k to 12k. Additionally, we report results from training on a 10k dataset constructed from FineCops-Ref. As expected, instruction tuning on FineCops-Ref yields better performance on this dataset. More interestingly, this also leads to improved performance on the other two compositional REC datasets, Ref-Adv and Ref-Reasoning. This highlights the advantage of FineCops-Ref over traditional RefCOCO datasets in terms of enhancing the reasoning capabilities required by MLLMs for handling complex REC tasks.

3) *Ablation on Variation in Number of Region Candidates in Instruction Tuning for CRS:* In the multi-choice instruction tuning process of CRS, the parameter k represents the number of candidate options. Specifically, the bounding boxes generated by Grounding DINO are ranked in descending order according to their confidence scores, and the top- k bounding boxes are selected as the final options. Table XI presents

TABLE XI: Ablation study of variation in the number of region candidates in instruction tuning for CRS. † denotes the use of multi-choice instruction tuning.

Model	Top-k	FineCops-Ref	Ref-Adv	Ref-Reasoning
Qwen2-VL-7B [52]	-	73.09	79.83	35.77
Qwen2-VL-7B†	Top-3	77.53	80.16	39.60
	Top-5	78.33	80.56	40.45
	Top-8	77.99	79.45	40.22
	Top-10	78.08	80.08	40.24

the experimental results, indicating that the method achieves optimal performance when top-5 candidates are adopted. This is due to the trade-off between recall and the introduction of distractors: while higher top- k values increase recall, they also bring in more irrelevant candidates. Setting $k=5$ strikes a better balance between improving recall and minimizing distractors. Therefore, we adopt a top- k value of 5 for our experimental settings.

VI. CONCLUSION

In this work, we introduced a high-quality dataset, FineCops-Ref, specifically designed for fine-grained compositional Referring Expression Comprehension (REC). This dataset incorporates varying difficulty levels and includes negative samples, providing a comprehensive evaluation of REC models’ capabilities in object detection, cross-modal reasoning, and rejection of non-existent objects—key aspects for real-world REC applications. To address these challenges, we proposed a Specialist-MLLM collaboration strategy that leverages the strengths of both object detection and cross-modal reasoning. This strategy is implemented through two approaches: Slow-Fast Adaptation (SFA), which dynamically assigns tasks to the appropriate specialist or MLLM model based on task difficulty, and Candidate Region Selection (CRS), which generates multiple region candidates using specialist models and selects the target through a multi-choice strategy. Extensive experiments on the FineCops-Ref dataset, along with two other challenging REC datasets, demonstrate the effectiveness of our proposed methods.

REFERENCES

- [1] L. Xiao, X. Yang, X. Lan, Y. Wang, and C. Xu, “Towards visual grounding: A survey,” *arXiv preprint arXiv:2412.20206*, 2024.
- [2] J. Mao, J. Huang, A. Toshev, O. Camburu, A. L. Yuille, and K. Murphy, “Generation and comprehension of unambiguous object descriptions,” in *CVPR*, 2016.

- [3] L. Yu, P. Poirson, S. Yang, A. C. Berg, and T. L. Berg, "Modeling context in referring expressions," in *ECCV*, 2016.
- [4] V. K. Nagaraja, V. I. Morariu, and L. S. Davis, "Modeling context between objects for referring expression understanding," in *ECCV*, 2016.
- [5] V. Cirik, L.-P. Morency, and T. Berg-Kirkpatrick, "Visual referring expression recognition: What do systems actually learn?" in *NAACL*, 2018.
- [6] A. Akula, S. Gella, Y. Al-Onaizan, S.-C. Zhu, and S. Reddy, "Words aren't enough, their order matters: On the robustness of grounding visual referring expressions," in *ACL*, 2020.
- [7] J. Liu, X. Yang, W. Li, and P. Wang, "Finecops-ref: A new dataset and task for fine-grained compositional referring expression comprehension," in *EMNLP*, 2024.
- [8] R. Liu, C. Liu, Y. Bai, and A. L. Yuille, "Clevr-ref+: Diagnosing visual reasoning with referring expressions," in *CVPR*, 2019.
- [9] Z. Chen, P. Wang, L. Ma, K.-Y. K. Wong, and Q. Wu, "Cops-ref: A new dataset and task on compositional referring expression comprehension," in *CVPR*, 2020.
- [10] S. Yang, G. Li, and Y. Yu, "Graph-structured referring expression reasoning in the wild," in *CVPR*, 2020.
- [11] D. A. Hudson and C. D. Manning, "Gqa: A new dataset for real-world visual reasoning and compositional question answering," in *CVPR*, 2019.
- [12] Y. Wu, Y. Wei, H. Wang, Y. Liu, S. Yang, and X. He, "Grounded image text matching with mismatched relation reasoning," in *ICCV*, 2023.
- [13] Y. Zeng, Y. Huang, J. Zhang, Z. Jie, Z. Chai, and L. Wang, "Investigating compositional challenges in vision-language models for visual grounding," in *CVPR*, 2024.
- [14] S. Kurita, N. Katsura, and E. Onami, "Refego: Referring expression comprehension dataset from first-person perception of ego4d," in *ICCV*, 2023.
- [15] S. Schuster, Y. Suh, K. M. Dafnis, Z. Zhang, S. Zhao, D. Metaxas *et al.*, "Omnilabel: A challenging benchmark for language-based object detection," in *ICCV*, 2023.
- [16] R. Hu, M. Rohrbach, J. Andreas, T. Darrell, and K. Saenko, "Modeling relationships in referential expressions with compositional modular networks," in *CVPR*, 2017.
- [17] H. Zhang, Y. Niu, and S.-F. Chang, "Grounding referring expressions in images by variational context," in *CVPR*, 2018.
- [18] B. Zhuang, Q. Wu, C. Shen, I. Reid, and A. Van Den Hengel, "Parallel attention: A unified framework for visual object discovery through dialogs and queries," in *CVPR*, 2018.
- [19] L. Yu, Z. Lin, X. Shen, J. Yang, X. Lu, M. Bansal, and T. L. Berg, "MATTNET: Modular attention network for referring expression comprehension," in *CVPR*, 2018.
- [20] X. Liu, Z. Wang, J. Shao, X. Wang, and H. Li, "Improving referring expression grounding with cross-modal attention-guided erasing," in *CVPR*, 2019.
- [21] S. Yang, G. Li, and Y. Yu, "Dynamic graph attention for referring expression comprehension," in *ICCV*, 2019.
- [22] R. Hong, D. Liu, X. Mo, X. He, and H. Zhang, "Learning to compose and reason with language tree structures for visual grounding," *TPAMI*, 2019.
- [23] D. Liu, H. Zhang, F. Wu, and Z.-J. Zha, "Learning to assemble neural module tree networks for visual grounding," in *ICCV*, 2019.
- [24] P. Wang, Q. Wu, J. Cao, C. Shen, L. Gao, and A. van den Hengel, "Neighbourhood watch: Referring expression comprehension via language-guided graph attention networks," in *CVPR*, 2018.
- [25] Y. Zhou, R. Ji, G. Luo, X. Sun, J. Su, X. Ding, C.-W. Lin, and Q. Tian, "A real-time global inference network for one-stage referring expression comprehension," *TNNLS*, 2021.
- [26] J. Deng, Z. Yang, T. Chen, W. Zhou, and H. Li, "Transvg: End-to-end visual grounding with transformers," in *ICCV*, 2021.
- [27] C. Zhu, Y. Zhou, Y. Shen, G. Luo, X. Pan, M. Lin, C. Chen, L. Cao, X. Sun, and R. Ji, "Seqtr: A simple yet universal network for visual grounding," in *ECCV*, 2022.
- [28] J. Deng, Z. Yang, D. Liu, T. Chen, W. Zhou, Y. Zhang, H. Li, and W. Ouyang, "Transvg++: End-to-end visual grounding with language conditioned vision transformer," *TPAMI*, 2023.
- [29] A. Kamath, M. Singh, Y. LeCun, G. Synnaeve, I. Misra, and N. Carion, "Mdetr-modulated detection for end-to-end multi-modal understanding," in *ICCV*, 2021.
- [30] B. Yan, Y. Jiang, J. Wu, D. Wang, P. Luo, Z. Yuan, and H. Lu, "Universal instance perception as object discovery and retrieval," in *CVPR*, 2023.
- [31] S. Liu, Z. Zeng, T. Ren, F. Li, H. Zhang, J. Yang, Q. Jiang, C. Li, J. Yang, H. Su *et al.*, "Grounding dino: Marrying dino with grounded pre-training for open-set object detection," in *ECCV*, 2024.
- [32] F. Shi, R. Gao, W. Huang, and L. Wang, "Dynamic mdetr: A dynamic multimodal transformer decoder for visual grounding," *TPAMI*, 2024.
- [33] N. Carion, F. Massa, G. Synnaeve, N. Usunier, A. Kirillov, and S. Zagoruyko, "End-to-end object detection with transformers," in *ECCV*, 2020.
- [34] X. Zhu, W. Su, L. Lu, B. Li, X. Wang, and J. Dai, "Deformable detr: Deformable transformers for end-to-end object detection," in *ICLR*, 2021.
- [35] H. Zhang, F. Li, S. Liu, L. Zhang, H. Su, J. Zhu, L. Ni, and H.-Y. Shum, "DINO: DETR with improved denoising anchor boxes for end-to-end object detection," in *ICLR*, 2023.
- [36] S. Zhao, L. Zhao, V. K. B. G, Y. Suh, D. N. Metaxas, M. Chandraker, and S. Schuster, "Generating enhanced negatives for training language-based object detectors," in *CVPR*, 2024.
- [37] L. Xiao, X. Yang, F. Peng, Y. Wang, and C. Xu, "Oneref: Unified one-tower expression grounding and segmentation with mask referring modeling," in *NeurIPS*, 2024.
- [38] M. Dai, L. Yang, Y. Xu, Z. Feng, and W. Yang, "Simvg: A simple framework for visual grounding with decoupled multi-modal fusion," in *NeurIPS*, 2024.
- [39] K. Chen, Z. Zhang, W. Zeng, R. Zhang, F. Zhu, and R. Zhao, "Shikra: Unleashing multimodal llm's referential dialogue magic," *arXiv preprint arXiv:2306.15195*, 2023.
- [40] H. You, H. Zhang, Z. Gan, X. Du, B. Zhang, Z. Wang, L. Cao, S.-F. Chang, and Y. Yang, "Ferret: Refer and ground anything anywhere at any granularity," in *ICLR*, 2024.
- [41] Z. Li, Q. Xu, D. Zhang, H. Song, Y. Cai, Q. Qi, R. Zhou, J. Pan, Z. Li, V. Tu, Z. Huang, and T. Wang, "GroundingGPT: Language enhanced multi-modal grounding model," in *ACL*, 2024.
- [42] F. Wei, X. Zhang, A. Zhang, B. Zhang, and X. Chu, "Lenna: Language enhanced reasoning detection assistant," *arXiv preprint arXiv:2312.02433*, 2023.
- [43] W. Wang, Q. Lv, W. Yu, W. Hong, J. Qi, Y. Wang, J. Ji, Z. Yang, L. Zhao, X. Song *et al.*, "Cogvlm: Visual expert for pretrained language models," in *NeurIPS*, 2024.
- [44] J. Qi, M. Ding, W. Wang, Y. Bai, Q. Lv, W. Hong, B. Xu, L. Hou, J. Li, Y. Dong *et al.*, "Cogcom: Train large vision-language models diving into details through chain of manipulations," *arXiv preprint arXiv:2402.04236*, 2024.
- [45] Z. Chen, W. Wang, H. Tian, S. Ye, Z. Gao, E. Cui, W. Tong, K. Hu, J. Luo, Z. Ma *et al.*, "How far are we to gpt-4v? closing the gap to commercial multimodal models with open-source suites," *Science China Information Sciences*, 2024.
- [46] J. Yang, H. Zhang, F. Li, X. Zou, C. Li, and J. Gao, "Set-of-mark prompting unleashes extraordinary visual grounding in gpt-4v," *arXiv preprint arXiv:2310.11441*, 2023.
- [47] H. Rasheed, M. Maaz, S. Shaji, A. Shaker, S. Khan, H. Cholakkal, R. M. Anwer, E. Xing, M.-H. Yang, and F. S. Khan, "Glamm: Pixel grounding large multimodal model," in *CVPR*, 2024.
- [48] H. Zhang, H. Li, F. Li, T. Ren, X. Zou, S. Liu, S. Huang, J. Gao, Leizhang, C. Li *et al.*, "Llava-grounding: Grounded visual chat with large multimodal models," in *ECCV*, 2024.
- [49] C. Ma, Y. Jiang, J. Wu, Z. Yuan, and X. Qi, "Groma: Localized visual tokenization for grounding multimodal large language models," in *ECCV*, 2024.
- [50] H. Shao, S. Qian, H. Xiao, G. Song, Z. ZONG, L. Wang, Y. Liu, and H. Li, "Visual cot: Advancing multi-modal language models with a comprehensive dataset and benchmark for chain-of-thought reasoning," in *NeurIPS*, 2024.
- [51] J. Li, D. Chen, Y. Hong, Z. Chen, P. Chen, Y. Shen, and C. Gan, "CoVLM: Composing visual entities and relationships in large language models via communicative decoding," in *ICLR*, 2024.
- [52] P. Wang, S. Bai, S. Tan, S. Wang, Z. Fan, J. Bai, K. Chen, X. Liu, J. Wang, W. Ge *et al.*, "Qwen2-vl: Enhancing vision-language model's perception of the world at any resolution," *arXiv preprint arXiv:2409.12191*, 2024.
- [53] Z. Chen, W. Wang, Y. Cao, Y. Liu, Z. Gao, E. Cui, J. Zhu, S. Ye, H. Tian, Z. Liu *et al.*, "Expanding performance boundaries of open-source multimodal models with model, data, and test-time scaling," *arXiv preprint arXiv:2412.05271*, 2024.
- [54] A. B. Yildirim, V. Baday, E. Erdem, A. Erdem, and A. Dundar, "Instinpaint: Instructing to remove objects with diffusion models," *arXiv preprint arXiv:2304.03246*, 2023.
- [55] Z. Ma, J. Hong, M. O. Gul, M. Gandhi, I. Gao, and R. Krishna, "Crepe: Can vision-language foundation models reason compositionally?" in *CVPR*, 2023.

- [56] C.-Y. Hsieh, J. Zhang, Z. Ma, A. Kembhavi, and R. Krishna, "Sugar-Crepe: Fixing Hackable Benchmarks for Vision-Language Compositionality," in *NeurIPS*, 2023.
- [57] Z. Lin, X. Chen, D. Pathak, P. Zhang, and D. Ramanan, "Revisiting the role of language priors in vision-language models," in *ICML*, 2024.
- [58] J. Zhuang, Y. Zeng, W. Liu, C. Yuan, and K. Chen, "A task is worth one word: Learning with task prompts for high-quality versatile image inpainting," in *ECCV*, 2024.
- [59] A. Radford, J. W. Kim, C. Hallacy, A. Ramesh, G. Goh, S. Agarwal, G. Sastry, A. Askell, P. Mishkin, J. Clark *et al.*, "Learning transferable visual models from natural language supervision," in *ICML*, 2021.
- [60] Z. Wang, J. Bao, W. Zhou, W. Wang, H. Hu, H. Chen, and H. Li, "Dire for diffusion-generated image detection," in *ICCV*, 2023.
- [61] M. Oquab, T. Darcet, T. Moutakanni, H. V. Vo, M. Szafraniec, V. Khalidov, P. Fernandez, D. HAZIZA, F. Massa, A. El-Nouby, M. Assran, N. Ballas, W. Galuba, R. Howes, P.-Y. Huang, S.-W. Li, I. Misra, M. Rabbat, V. Sharma, G. Synnaeve, H. Xu, H. Jegou, J. Mairal, P. Labatut, A. Joulin, and P. Bojanowski, "DINOv2: Learning robust visual features without supervision," *TMLR*, 2024.
- [62] X. Zhao, Y. Chen, S. Xu, X. Li, X. Wang, Y. Li, and H. Huang, "An open and comprehensive pipeline for unified object grounding and detection," *arXiv preprint arXiv:2401.02361*, 2024.
- [63] J. Achiam, S. Adler, S. Agarwal, L. Ahmad, I. Akkaya, F. L. Aleman, D. Almeida, J. Altschmidt, S. Altman, S. Anadkat *et al.*, "Gpt-4 technical report," *arXiv preprint arXiv:2303.08774*, 2023.
- [64] E. Mitchell, Y. Lee, A. Khazatsky, C. D. Manning, and C. Finn, "Detectgpt: Zero-shot machine-generated text detection using probability curvature," in *ICML*, 2023.
- [65] H. Wang, P. Ren, Z. Jie, X. Dong, C. Feng, Y. Qian, L. Ma, D. Jiang, Y. Wang, X. Lan *et al.*, "Ov-dino: Unified open-vocabulary detection with language-aware selective fusion," *arXiv preprint arXiv:2407.07844*, 2024.
- [66] J. Jeong, G. Park, J. Yoo, H. Jung, and H. Kim, "Proxydet: Synthesizing proxy novel classes via classwise mixup for open-vocabulary object detection," in *AAAI*, 2024.
- [67] T. Cheng, L. Song, Y. Ge, W. Liu, X. Wang, and Y. Shan, "Yolo-world: Real-time open-vocabulary object detection," in *CVPR*, 2024.